Presti, F. T., Pace, R. J., & Chan, S. I. (1982) *Biochemistry 21*, 3831–3835.
Rogers, J., Lee, A. G., & Wilton, D. C. (1979) *Biochim. Biophys. Acta 552*, 23–37.
Rooney, M. W., Lange, Y., & Kauffman, J. W. (1984) *J. Biol. Chem. 259*, 8281–8285.
Sarzala, M. G., Pilarska, M., Zubrycka, E., & Michalak, M. (1975) *Eur. J. Biochem. 57*, 25–34.
Schindler, H. (1982) *Neurosci. Res. Program Bull. 20*, 295–301.
Schubert, D., & Boss, K. (1982) *FEBS Lett. 150*, 4–8.
Scotto, A. W., & Zakim, D. (1986) *Biochemistry 25*, 1555–1561.
Silvius, J. R., McMillen, D. A., Saley, N. D., Jost, P. C., & Griffith, O. H. (1984) *Biochemistry 23*, 538–547.
Simmonds, A. C., East, J. M., Jones, O. T., Rooney, E. K., McWhirter, J., & Lee, A. G. (1982) *Biochim. Biophys. Acta 693*, 398–406.
Simmonds, A. C., Rooney, E. K., & Lee, A. G. (1984) *Biochemistry 23*, 1432–1441.
Singer, S. J., & Nicholson, G. L. (1972) *Science (Washington, D.C.) 175*, 720–731.
Spencer, R. D., & Weber, G. (1969) *Ann. N.Y. Acad. Sci. 158*, 361–376.
Tefft, R. E., Jr., Carruthers, A., & Melchior, D. L. (1986) *Biochemistry 25*, 3709–3718.
Tietz, N. W. (1970) *Fundamentals of Clinical Chemistry*, pp 860–864, Saunders, Philadelphia.
Warren, G. B., Houslay, M. D., Metcalfe, J. C., & Birdsall, N. J. M. (1975) *Nature (London) 255*, 684–687.
Yeagle, P. L. (1985) *Biochim. Biophys. Acta 822*, 267–287.

Mechanism of Agonist and Antagonist Binding to α_2 Adrenergic Receptors: Evidence for a Precoupled Receptor–Guanine Nucleotide Protein Complex†

Richard R. Neubig,*,‡,§ Robin D. Gantzos,‡ and William J. Thomsen‡
Department of Pharmacology and Department of Internal Medicine, The University of Michigan, Ann Arbor, Michigan 48109-0010
Received May 14, 1987; Revised Manuscript Received November 19, 1987

ABSTRACT: The α_2 adrenergic receptor (AR) inhibits adenylate cyclase via an interaction with N_i, a guanine nucleotide binding protein. The early steps involved in the activation of the α_2 AR by agonists and the subsequent interaction with N_i are poorly understood. In order to better characterize these processes, we have studied the kinetics of ligand binding to the α_2 AR in human platelet membranes on the second time scale. Binding of the α_2 antagonist [^{3}H]yohimbine was formally consistent with a simple bimolecular reaction mechanism with an association rate constant of 2.5×10^5 M^{-1} s^{-1} and a dissociation rate constant of 1.11×10^{-3} s^{-1}. The low association rate constant suggests that this is not a diffusion-limited reaction. Equilibrium binding of the α_2 adrenergic full agonist [^{3}H]UK 14 304 was characterized by two binding affinities: K_{d1} = 0.3–0.6 nM and K_{d2} = 10 nM. The high-affinity binding corresponds to approximately 65% and the low-affinity binding to 35% of the total binding. The kinetics of binding of [^{3}H]UK 14 304 were complex and not consistent with a mass action interaction at one or more independent binding sites. The dependence of the kinetics on [^{3}H]UK 14 304 concentration revealed a fast phase with an apparent bimolecular reaction constant k_+ of 5×10^6 M^{-1} s^{-1}. The rate constants and amplitudes of the slow phase of agonist binding were relatively independent of ligand concentration. These results were analyzed quantitatively according to several variants of the "ternary complex" binding mechanism. In the model which best accounted for the data, (1) approximately one-third of the α_2 adrenergic receptor binds agonist with low affinity and is unable to couple with a guanine nucleotide binding protein (N protein), (2) approximately one-third is coupled to the N protein prior to agonist binding, and (3) the remainder interacts by a diffusional coupling of the α_2 AR with the N protein or a slow, ligand-independent conformational change of the α_2 AR–N protein complex. The rates of interaction of liganded and unliganded receptor with N protein are estimated.

The study of the mechanism of activation and inhibition of adenylate cyclase by hormone receptors has shown remarkable progress recently (Gilman, 1984). Resolution, purification, and reconstitution of the individual proteins involved in these reactions has recently been achieved (Asano et al., 1984; May et al., 1985; Cerione et al., 1986). These advances allow detailed study of the interactions of the individual components in a well-defined system. To understand the implications of such interactions in reconstituted systems with respect to a less perturbed membrane environment, it would be useful to have probes that would be applicable in both systems. Extensive studies of adenylate cyclase activity in native membranes have resulted in models of the interaction of receptor (R)[1] and

† This work was supported by NSF Grant DCB-8409333. R.R.N. is a Hartford Fellow; W.J.T. is a Horace H. Rackham Predoctoral Fellow.
* Address correspondence to this author at the Department of Pharmacology, M6322 Medical Science Bldg. I, Ann Arbor, MI 48109-0626.
‡ Department of Pharmacology.
§ Department of Internal Medicine.

[1] Abbreviations: AR, adrenergic receptor; C, catalytic subunit of adenylate cyclase; GppNHp, guanosine 5′-(β,γ-imidotriphosphate); N_i, inhibitory guanine nucleotide binding protein; N protein, guanine nucleotide binding protein; UK 14 304, 5-bromo-*N*-(4,5-dihydroimidazol-2-yl)-6-quinoxalinamine; R, receptor; SS, sum of squared residuals; Tris-HCl, tris(hydroxymethyl)aminomethane hydrochloride; EGTA, ethylene glycol bis(β-aminoethyl ether)-*N,N,N′,N′*-tetraacetic acid.

0006-2960/88/0427-2374$01.50/0

guanine nucleotide binding protein (N) with the catalytic subunit of adenylate cyclase (C) (Ross et al., 1977). In particular, analysis of the transient kinetics of adenylate cyclase activation and inhibition have proved enlightening (Tolkovsky & Levitzki, 1978; Jakobs & Aktories, 1983). Kinetic studies of the effects of adrenergic agonists on guanine nucleotide binding and release have also been used in both native (Michel & Lefkowitz, 1982; Motulsky & Insel, 1983; Murayami & Ui, 1984) and reconstituted (Asano & Ross, 1984; Brandt & Ross, 1986) systems.

Equilibrium radioligand binding studies with high-affinity, high specific activity antagonist compounds are widely applicable and have substantially advanced our understanding of receptor mechanisms. By use of radiolabeled antagonists in competition experiments, the equilibrium binding of agonists can also be determined indirectly (Stiles et al., 1984) as can the kinetics (Motulsky & Mahan, 1984). Recent studies of the time dependence of adrenergic agonist binding to whole cells have used these competition techniques (Toews et al., 1983; Insel et al., 1984; Hoyer et al., 1984; Schwartz et al., 1985, 1987). An approach that has been successfully applied to studies of the nicotinic acetylcholine receptor is the detailed kinetic analysis of *direct* measurements of radiolabeled and fluorescent agonist binding as a marker for conformational transitions of that receptor (Boyd & Cohen, 1980a,b; Neubig et al., 1982; Heidmann et al., 1983). Even transiently populated receptor states may be detected by this technique. Similar kinetic approaches have been used in the analysis of binding of the antagonists QNB (Galper & Smith, 1979) and IHYP (Ross et al., 1977) to muscarinic and adrenergic receptors, respectively, and to glucagon (Horowitz et al., 1985) and nitrendipine (Weiland & Oswald, 1985) binding to their receptors. Remarkably few studies of direct measurements of adrenergic agonist binding kinetics have been reported [see DeLean et al. (1983)], possibly because of the lack of suitable radioligands. The α_2 adrenergic receptor has been an exception in that clonidine derivatives, which are partial agonists, have proved very useful in direct binding studies (U'Prichard et al., 1983). The equilibrium binding of an imidazoline α_2 adrenergic full agonist, [^{3}H]UK 14 304, has recently been characterized by ourselves (Neubig et al., 1985) and others (Loftus et al., 1984; Turner et al., 1985). The availability of this radioligand and a partially purified plasma membrane preparation from human platelets that is enriched in α_2 adrenergic receptors (Neubig & Szamraj, 1986) facilitates the study of α_2 agonist binding kinetics. In addition, reconstitution studies using purified guanine nucleotide binding proteins have established the role of N proteins in the high-affinity binding of α_2 agonists in this system (Kim & Neubig, 1987).

This paper reports the first detailed kinetic analysis of radiolabeled adrenergic agonist binding in membranes. The results are consistent with a model in which approximately one-third of the α_2 receptor is unable to couple to N_i. Of the remainder, approximately half of the receptor is coupled to N_i prior to agonist binding and the other half becomes coupled after agonist is present. Parameters for the interaction of the liganded and unliganded α_2 AR with the N protein are estimated. This approach of studying direct agonist binding should prove useful for further studies of factors that affect receptor–N protein interactions.

Experimental Procedures

Purified platelet plasma membranes were prepared from human platelet concentrates as described by Neubig and Szamraj (1986) and stored for up to 6 weeks at −70 °C. Preparations used in these studies contained approximately 400–1300 fmol of [^{3}H]yohimbine binding sites per milligram of protein.

Radioligands. [^{3}H]Yohimbine (75–85 Ci/mmol) and [^{3}H]UK 14 304 (77–88 Ci/mmol) were obtained from New England Nuclear. In some experiments using high concentrations of radioligands, specific activities were reduced 2–8-fold by dilution with nonradioactive ligand.

Equilibrium binding measurements were performed in buffer containing 50 mM Tris-HCl, 10 mM $MgCl_2$, and 1 mM EGTA, pH 7.6, essentially as described by Neubig et al. (1985). In brief, binding of [^{3}H]yohimbine was measured following incubation for 30–60 min at 23 °C in a reaction volume of 0.1 mL (1–2 mg of protein/mL). Equilibrium binding of [^{3}H]UK 14 304 was measured following incubation for 60–90 min at 23 °C in a reaction volume of 1.0 mL (0.1–0.3 mg of protein/mL) unless otherwise specified. For experiments involving [^{3}H]UK 14 304 concentrations of 10 nM and above, the GF/C filters were soaked in 0.03% poly(ethylenimine) to reduce nonspecific binding (Bruns et al., 1983; Neubig et al., 1985).

Binding Kinetics. The time course of association of radioligands was measured by mixing equal volumes of the platelet membranes and radioligand in a manual syringe mixer as described (Boyd & Cohen, 1980a; Neubig et al., 1985). Reagents were preequilibrated for 3–5 min in a water bath at 23–25 °C prior to initiating the reaction. The dependence of nonspecific binding on time of incubation was similarly determined by adding excess nonradioactive ligand (10^{-5} M yohimbine or oxymetazoline) to the receptor-rich membranes prior to the preequilibration period. Specific binding was calculated by subtracting from the total binding the nonspecific binding estimated for the same time by a linear least-squares fit of the nonspecific binding data. Specific binding represented at least 80% of the total [^{3}H]yohimbine binding at all times greater than 1 min. For [^{3}H]UK 14 304, specific binding accounted for greater than 50% of total binding at 1 min for all concentrations. At the later time points and at equilibrium, specific binding of [^{3}H]UK 14 304 accounted for 75–95% of total binding at low concentrations (0.1–3 nM) and 50–70% at higher concentrations.

Dissociation kinetics were determined by allowing radioligand and α_2 receptor rich membranes to reach equilibrium (as indicated above) followed by addition of a small volume of nonradioactive ligand (1% of total). Aliquots were removed at the indicated times for determination of specific binding. Nonspecific binding was determined in parallel samples pretreated with nonradioactive ligand prior to addition of radioligand and incubated for the same total amount of time as the samples for measuring total ligand binding. For [^{3}H]UK 14 304, more than 95% of specific binding had dissociated by 6 h after addition of competing agonist.

Analysis of Data. Semilogarithmic plots of specific binding were prepared for association kinetics by plotting ln $[B_{eq}/(B_{eq} - B_t)]$ versus time. B_{eq} is specific binding at equilibrium; B_t is specific binding at time t. The slope of such a plot, k_{obsd}, is the observed rate constant. This method is valid under the pseudo-first-order conditions of these experiments in which no more than 10% of the total radioligand is bound (Weiland & Molinoff, 1981). Essentially the same results were obtained with a nonlinear least-squares fit to a single exponential function. Experiments for which semilogarithmic plots were not linear were also analyzed by EXPFIT, a nonlinear least-squares parameter estimation program for fitting multiple exponential processes (Faden & Rodbard, 1975).[2] Most

Chart I: Models of Agonist Binding Kinetics[a]

(I) Two Independent Receptors

$$D + R' \underset{k_{-1}'}{\overset{k_1'}{\rightleftharpoons}} DR'$$

$$D + R \underset{k_{-1}}{\overset{k_1}{\rightleftharpoons}} DR$$

(II) Two Receptors with Ligand-Dependent Receptor Conformational Change or RN Coupling

$$D + R' \underset{k_{-1}'}{\overset{k_1'}{\rightleftharpoons}} DR'$$

$$D + R \underset{k_{-1}}{\overset{k_1}{\rightleftharpoons}} DR \overset{N\ k_2}{\underset{k_{-2}}{\rightleftharpoons}} DRN$$

(III) Two Receptors with Ligand-Independent Conformational Change or RN Coupling

$$D + R' \underset{k_{-1}'}{\overset{k_1'}{\rightleftharpoons}} DR'$$

$$R \quad N\ k_4 \uparrow\downarrow k_{-4}$$

$$D + RN \underset{k_{-3}}{\overset{k_3}{\rightleftharpoons}} DRN$$

(IV) Ternary Complex with Distinct Uncoupled Receptor

$$D + R' \underset{k_{-1}'}{\overset{k_1'}{\rightleftharpoons}} DR'$$

$$D + R \underset{k_{-1}}{\overset{k_1}{\rightleftharpoons}} DR \qquad N\ k_4 \uparrow\downarrow k_{-4} \qquad N\ k_2 \uparrow\downarrow k_{-2}$$

$$D + RN \underset{k_{-3}}{\overset{k_3}{\rightleftharpoons}} DRN$$

[a] Several models used to analyze the [^{3}H]UK 14 304 binding kinetics are shown. R represents the α_2 receptor, D the radioligand, and DR the ligand–receptor complex. N represents a guanine nucleotide binding protein. k_n and k_{-n} are the forward and backward rate constants, respectively, for the nth reaction step. R and R′ represent two distinct noninterconvertible forms of the receptor. These may differ in structure or simply in their accessibility to coupling proteins. The receptor designated R′ is associated with the low-affinity non-GTP-sensitive equilibrium binding. The receptor conformation binding agonist with high affinity in these models is designated RN because of biochemical (Smith & Limbird, 1981) and reconstitution (Kim & Neubig, 1987) evidence for α_2 receptor–N protein complexes.

[^{3}H]UK 14 304 association experiments were fit best by a model with two exponential components (four parameter) or by a model with two exponentials and a constant term (five parameter). The [^{3}H]UK 14 304 dissociation kinetics were also most often fit best by a four-parameter model. The values from the four-parameter fit were always used for subsequent analysis. The rate constants for the two exponential binding components and the percentage of the binding reaction that occurred during the fast phase of binding were plotted against radioligand concentration. These secondary plots were used for comparison to theoretical results predicted for different models of receptor binding.

Theoretical Models of Binding Kinetics and Nonlinear Regression Analysis. Data were analyzed according to the models listed in Chart I. For the models with simple bimolecular binding mechanisms (including either single or multiple binding sites), predicted rate constants were determined according to the relation

$$k_{obsd} = k_- + k_+[D] \qquad (1)$$

The term k_- is the unimolecular dissociation rate constant, k_+ is the bimolecular association rate constant, [D] is the free drug concentration, and k_{obsd} is the observed rate constant. Simulations of ligand binding kinetics in the more complex models were initially performed with an Euler's method computer program written in Basic for an IBM PC computer to solve the differential equations numerically. After initial estimates of the parameters were obtained by comparison of predicted secondary plots with those observed, parameter refinement and statistical comparisons of the models were done with SAAM 29 (Boston et al., 1981). Comparisons of the models were done by an F test to correct for additional free parameters as described (Rodbard, 1974).

Miscellaneous. Protein was determined by the method of Lowry et al. (1951) with bovine albumin as a standard. Oxymetazoline and UK 14 304 tartrate were kind gifts of Schering Co. and Pfizer Co., respectively. l-Epinephrine, yohimbine, and guanine nucleotides were from Sigma. All other chemicals were of reagent grade or better from commercial suppliers.

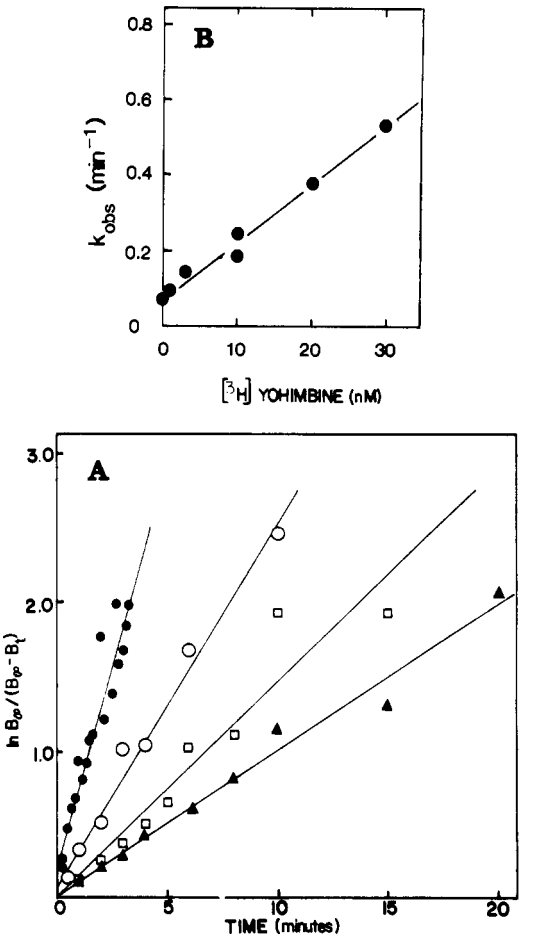

FIGURE 1: Time course of [^{3}H]yohimbine binding. (A) Semilogarithmic plot of specific [^{3}H]yohimbine binding at concentrations of 1 (▲), 3 (□), 10 (○), and 30 nM (●). B_{eq} is specific binding at equilibrium (60 min), and B_t is specific binding at the indicated time. The lines are linear least-squares fits of the data. (B) Observed rates of [^{3}H]yohimbine binding, k_{obsd}, were determined from the slopes of lines in (A) and similar experiments and are plotted against concentration of radioligand. For each concentration of [^{3}H]yohimbine (except 20 nM), two or three determinations of k_{obsd} were done with values differing by less than the symbol size unless indicated.

[2] This method of analysis of binding kinetics by exponential decomposition is simply descriptive; it does not assume any specific binding mechanism. As in studies of chemical kinetics (Czerlinski, 1966), mechanistic information is obtained by observing the variation in the rates and amplitudes of the exponential phases with reactant concentration.

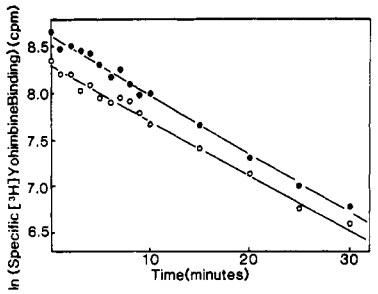

FIGURE 2: Equilibrium and preequilibrium dissociation of [^{3}H]yohimbine. [^{3}H]Yohimbine (30 nM final) and platelet plasma membranes were mixed at 23 °C, and specific binding was determined at 2, 2.5, and 3 min. To determine preequilibrium dissociation, excess nonradioactive yohimbine (10^{-5} M) was added to half of the reaction mixture at 2.5 min. Specific binding was determined at the indicated times after addition of cold ligand (○). The value indicated for zero time was the average of the specific binding determined at 2, 2.5, and 3 min. Specific binding at equilibrium was determined 60 min after addition of [^{3}H]yohimbine. Dissociation was then initiated as above and specific binding determined at the indicated times following addition of cold ligand (●). Values are means of duplicate determinations from one experiment representative of four similar experiments. Lines are linear least-squares fits of the data with slopes of 1.07×10^{-3} (●) and 0.97×10^{-3} (○) s^{-1}.

RESULTS

[^{3}H]Yohimbine Binding Kinetics. The time course of [^{3}H]yohimbine binding is strongly dependent on ligand concentration in the range of 1–30 nM, and semilogarithmic plots are linear to at least 90% of the extent of reaction, indicating an exponential approach to equilibrium (Figure 1A). Rate constants (k_{obsd}) for [^{3}H]yohimbine binding at the various concentrations were determined from linear least-squares fits of the transformed data. A secondary plot of k_{obsd} versus [^{3}H]yohimbine concentration is also linear (Figure 1B). The forward bimolecular rate constant, k_+, calculated from the slope of this line is 1.52×10^7 M^{-1} min^{-1} or 2.5×10^5 M^{-1} s^{-1}. This rate constant is significantly less than the 10^8–10^9 M^{-1} s^{-1} expected for a simple diffusion-controlled reaction (Ferscht, 1977). The intercept of the secondary plot is 1.2×10^{-3} s^{-1}, which is in good agreement with the directly measured dissociation rate constant, $(1.11 \pm 0.08) \times 10^{-3}$ s^{-1} ($n = 7$). The corresponding $T_{1/2}$ of 10.4 min is consistent with previous reports, as is the calculated K_d of 4.8 nM (U'Prichard et al., 1983; Garcia-Sevilla et al., 1981).

[^{3}H]Yohimbine dissociation was also determined prior to equilibration of the radioligand. Both equilibrium and preequilibrium dissociation were exponential and exhibited virtually identical rate constants, 1.07×10^{-3} and 0.97×10^{-3} s^{-1}, respectively (Figure 2). There was no evidence for a rapid phase of dissociation to suggest a low-affinity preequilibrium complex as has been described for [^{3}H]QNB binding to the muscarinic receptor (Galper & Smith, 1979). GppNHp (10^{-5} M) did not affect the kinetics of either association or dissociation of [^{3}H]yohimbine (data not shown).

Equilibrium Binding of [^{3}H]UK 14 304. We have extended our previous studies of the equilibrium binding of the α_2 adrenergic full agonist [^{3}H]UK 14 304 (Neubig et al., 1985) to both higher and lower concentrations (0.01–100 nM) to better define the binding parameters. Figure 3 shows Scatchard plots of [^{3}H]UK 14 304 binding at concentrations of 0.01–2 nM (Figure 3A) and 0.2–100 nM (Figure 3B). The high-affinity K_d was 0.46 ± 0.13 nM in seven experiments similar to that in Figure 3A with membranes diluted or washed to remove contaminating guanine nucleotides. In our previous experiments with ligand concentrations up to 30 nM, the low-affinity

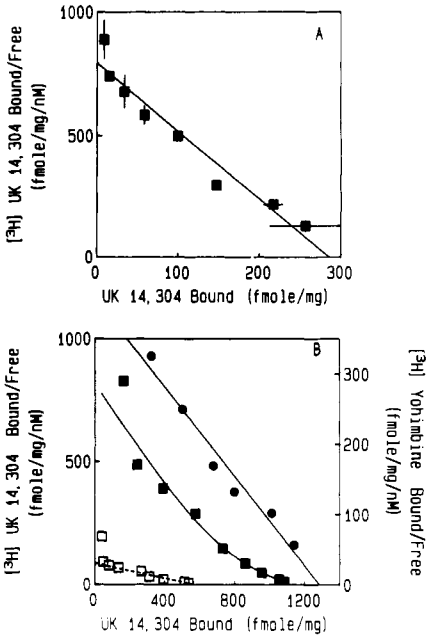

FIGURE 3: Equilibrium binding of [^{3}H]UK 14 304. (A) Platelet membranes (0.156 mg of protein) were incubated in 10 mL of TME buffer with 0.01–2.0 nM [^{3}H]UK 14 304 for 90 min at 25 °C. Specific binding was measured as described under Materials and Methods. A Scatchard transformation of the data is shown with values expressed as mean ± SD of triplicate determinations. The solid line is a linear least-squares fit of the data after Scatchard transformation. This membrane preparation contained 460 fmol/mg of [^{3}H]yohimbine binding sites (B_{max}). (B) Specific binding of [^{3}H]UK 14 304 (0.2–100 nM) was measured in 1-mL aliquots containing 0.118–0.150 mg of protein in the absence (■) and presence (□) of 10^{-5} M GppNHp. Data in the absence of nucleotide are averages of three experiments on a single membrane preparation each with duplicate determinations, and binding in the presence of GppNHp is from a single experiment with duplicate determinations. Binding of [^{3}H]yohimbine to the same preparation is shown (●). Solid lines are nonlinear least-squares fits of the data with parameters discussed in the text. The specific activity of [^{3}H]UK 14 304 was reduced to 18.8 Ci/mmol by isotropic dilution.

K_d for [^{3}H]UK 14 304 could not be reliably determined. In more highly enriched preparations of platelet membranes (800–1300 fmol/mg of [^{3}H]yohimbine binding sites), it has been possible to extend these studies to higher concentrations of radioligand. By use of poly(ethylenimine)-treated filters, specific binding was 53–60% of total binding at 100 nM, the highest concentration used in Figure 3B. Also, we have recently shown that, with 100 nM [^{3}H]UK 14 304, the same value of nonspecific binding is obtained when three specific drugs of very distinct structure as the competing ligand are used: 10 μM oxymetzoline, 10 μM yohimbine, and 100 μM l-epinephrine (Neubig & Thomsen, 1987). A nonlinear least-squares fit of the combined data from three experiments gave K_d values of 0.9 ± 0.3 nM and 9.9 ± 7.8 nM for the high- and low-affinity binding, respectively. The estimated B_{max} values were 700 ± 210 and 430 ± 190 fmol/mg, respectively. In the presence of 10 μM GppNHp, [^{3}H]UK 14 304 binding was markedly reduced and was characterized by a K_d of 6.8 nM and a B_{max} of 560 fmol/mg. The total [^{3}H]UK 14 304 binding (1130 fmol/mg) was slightly less than the B_{max} of 1280 fmol/mg observed for [^{3}H]yohimbine in this membrane preparation.

[^{3}H]UK 14 304 Association Kinetics. Detailed studies of the time course of [^{3}H]UK 14 304 binding were performed over a 300-fold concentration range, 0.1–30 nM. Semilogarithmic plots of specific binding versus time are distinctly nonlinear (Figure 4). This is in contrast to the linear semilogarithmic plots for the antagonist [^{3}H]yohimbine

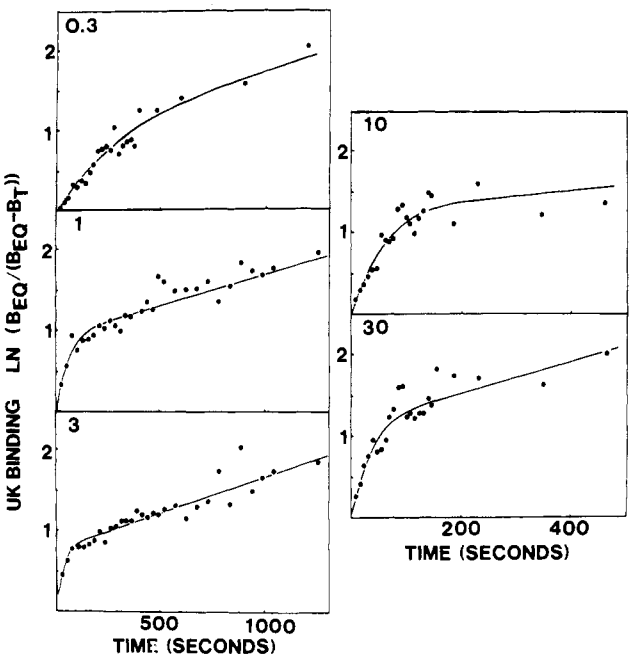

FIGURE 4: Semilogarithmic plots of [^{3}H]UK 14 304 association kinetics. Specific binding of [^{3}H]UK 14 304 at 23 °C was determined as described in Figure 3 and under Materials and Methods. Semilogarithmic plots of specific binding are shown for the indicated [^{3}H]UK 14 304 concentrations from 0.3 to 30 nM. B_{eq} represents specific binding at equilibrium, and B_t is specific binding at the indicated time. Values for times up to 5 min are individual determinations while later times are means of duplicate determinations. Equilibrium points were determined in triplicate. All experiments were performed with the same preparation of human platelet plasma membranes. Solid lines are nonlinear least-squares fits of the data to the two-exponential model with EXPFIT.

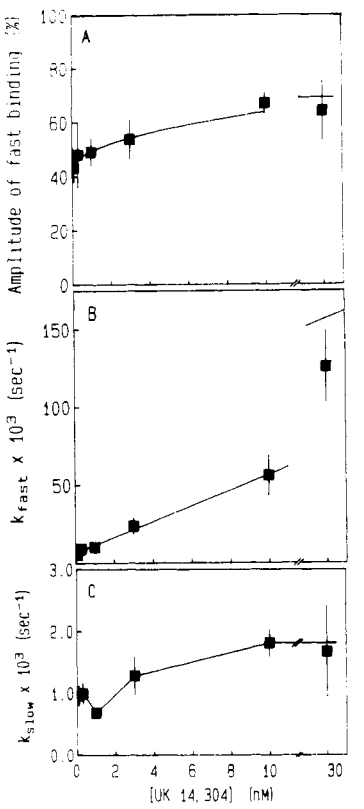

FIGURE 5: Dependence of amplitudes and rate constants of [^{3}H]UK 14 304 association kinetics on ligand concentration. Plots are shown of (A) A_f, the percent of binding occurring during the fast phase, (B) k_f, the rate constant of the fast phase, and (C) k_s, the rate constant of the slow phase versus [^{3}H]UK 14 304 concentration. Values were determined from the results of nonlinear least-squares analysis of association kinetics with EXPFIT as illustrated in Figure 4. Data are mean ± SEM of three to seven experiments.

(Figure 1A). The time course of [^{3}H]UK 14 304 binding was fit to two exponential phases of binding (see Materials and Methods).[2] Qualitative inspection of the semilogarithmic plots reveals that the rate of the fast component of binding increases steadily with concentration (Figure 4). In contrast, the rate of the slow phase as indicated by the slope of the semilogarithmic plots at later times is relatively independent of ligand concentration over the entire range of concentrations. These observations are confirmed when parameter estimates of the rate constants for the fast and slow phases of binding are determined by a nonlinear least-squares regression method (Figure 5B,C). The plots of association rates, k_f and k_s, were initially analyzed according to the usual mass action model with eq 1. The rate constant for the fast phase of binding, k_f, increases linearly with concentration, consistent with a bimolecular reaction mechanism (see below). The slope of the secondary plot (i.e., the association rate constant) is 5.0 × 10^6 M^{-1} s^{-1}. The intercept is 6.5 × 10^{-3} s^{-1}, and the calculated equilibrium dissociation constant is 1.3 nM, which is similar to the previously reported equilibrium K_d of 0.9 nM (Neubig et al., 1985). Analysis of the slow rates, k_s, revealed a slope of 2.7 × 10^4 M^{-1} s^{-1} and an intercept of 1.03 × 10^{-3} s^{-1}. The calculated equilibrium dissociation constant was 38 nM. Although these values appear to agree relatively well with the measured equilibrium K_d's (Figure 3), there are several facts suggesting that more complicated mechanisms are involved. First, the slow component of [^{3}H]UK 14 304 binding appears to be associated with the high-affinity equilibrium binding (Loftus et al., 1984; Turner et al. 1985) rather than the low-affinity binding predicted by this analysis. Second, the amplitudes of the fast and slow phases of agonist binding are not consistent with the mass action parameters. A model

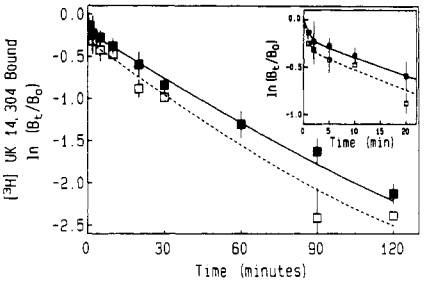

FIGURE 6: Dissociation of [^{3}H]UK 14 304 from washed platelet membranes. [^{3}H]UK 14 304 [(■) 0.1 and (□) 30 nM] was incubated with platelet membranes for 90 min at 24 °C and then 10^{-5} M oxymetazoline was added to initiate dissociation. One-milliliter aliquots were filtered at the indicated times, and specific binding, B_t, was calculated as described under Materials and Methods. B_0 was specific binding just prior to adding nonradioactive ligand and is 420–450 cpm for 0.1 nM and 2800–3000 cpm for 30 nM [^{3}H]UK 14 304. Nonspecific binding is 40–50 cpm for 0.1 nM and 1300–1600 cpm for 30 nM radioligand.

in which fast binding is to receptor with high affinity for agonist and the slow binding is to low-affinity receptor would predict a *decrease* in the percentage of fast binding, A_f, from 95 to 60% with increasing ligand concentration rather than the increase observed here.

[^{3}H]UK 14 304 Dissociation Kinetics. Dissociation of [^{3}H]UK 14 304 at equilibrium (90 min at 23 °C) was measured for ligand concentrations of 0.1, 0.3, 1, 3, 10, and 30 nM. There was no consistent difference in dissociation kinetics for the various ligand concentrations, and biphasic kinetics were always observed (Figure 6). More than 95% of the

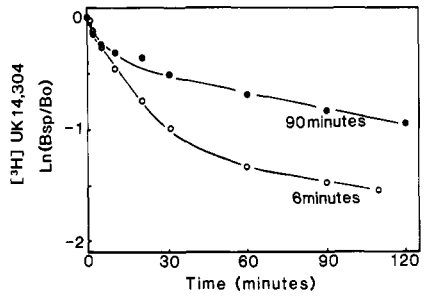

FIGURE 7: Preequilibrium dissociation of [^{3}H]UK 14 304. Platelet plasma membranes (10.8 mg of protein) were washed after thawing by resuspension in 60 mL of TME buffer followed by centrifugation for 30 min at 160000g at 4 °C. Following resuspension to 0.264 mg/mL and warming to 23 °C, an equal volume of 2 nM [^{3}H]UK 14 304 was added. After 6 (○) or 90 (●) min, 10^{-5} M oxymetazoline was added, and dissociation kinetics was determined. B_0 was determined from equilibrium binding [2079 cpm (●)] or by interpolation of specific binding obtained at 5 and 7 min [995 cpm (○)].

specific binding dissociated by 6 h, indicating that virtually all of the binding of [^{3}H]UK 14 304 was reversible. Approximately one-fourth of the binding dissociated rapidly (range 19–32%) with half-times of 30–70 s (k_{off} = 0.010–0.022 s^{-1}). Although the rates of the rapid dissociation are not precisely specified by the data, the amplitude (or percentage) of fast dissociation can be accurately determined from the y intercept of the slowly dissociating component on semilogarithmic plots. The remainder of the binding dissociated slowly with half-times of 28–40 min [k_{off} = (2.8–4.3) × 10^{-4} s^{-1}]. These dissociation kinetics provide additional evidence against the simple two-receptor model. The amount of slowly dissociating ligand (70–80%) is similar to the amount of rapidly associating ligand (60–70%) at 1 nM [^{3}H]UK 14 304. The rate constants determined from the mass action analysis predict that the rapidly associating ligand should also dissociate rapidly. This discrepancy is best resolved by postulating conformational changes in the receptor that lead to slow agonist dissociation (see below for specific models).

Dissociation of [^{3}H]UK 14 304 prior to equilibrium was also studied (Figure 7). After 6 min of association, a time at which almost all of the binding corresponds to the fast component, 56 ± 5% (n = 3) of the binding dissociated rapidly while in the same experiments only 35 ± 8% dissociated fast at equilibrium. Faster dissociation of ligand prior to equilibration has been observed also for binding of QNB (Galper & Smith, 1979), IHYP (Ross et al., 1977), ^{125}I-glucagon (Horowitz et al., 1985), and δ-opiate agonists (Spain & Coscia, 1987). In all of those cases models were proposed in which an initial weak binding interaction resulted in a conformational isomerization of the receptor to a form with a higher affinity and a slower dissociation rate.

Nonlinear Least-Squares Analysis of [^{3}H]UK 14 304 Binding Kinetics. Because of discrepancies between predictions of the simple two receptor model and our data, we have analyzed our results according to several additional models. We used the SAAM kinetic analysis package to perform nonlinear least-squares fits of the data in order to (1) determine which model best accounts for our data and (2) obtain quantitative estimates of the rate parameters.

The choice of models to use in this analysis was based on previous models used for such receptor systems and on our current data. The ternary complex model of DeLean et al. (1980) has been used widely to analyze the equilibrium binding of agonists to N protein coupled receptors. Also, substantial biochemical data support its applicability to platelet α_2 receptors (Smith & Limbird, 1981; Michel et al., 1981; Kim & Neubig, 1987). However, the ternary complex model as originally formulated cannot account for the complex equilibrium binding of [^{3}H]UK 14 304 given the measured 50–100-fold excess of N_i over α_2 receptors in human platelet plasma membranes (Neubig et al., 1985). It has been pointed out that to account for nonhyperbolic equilibrium binding there must be nearly equal amounts of receptor and coupling protein (Wreggett & DeLean, 1984; Neubig et al., 1985; Ehlert, 1985; Lee et al., 1986), so one must invoke structural heterogeneity or functional compartmentation of the α_2 receptor or N protein to account for the observed equilibrium binding of α_2 agonists in platelet membranes. Severne et al. (1987) have come to similar conclusions regarding the β_2 adrenergic receptor in bovine muscle. Thus the models we discuss to account for the [^{3}H]UK 14 304 association and dissociation kinetics include two or more populations of receptor.

The simplest such model (model I in Chart I) consists of two independent receptors with mass action mechanisms. Even though model I cannot account for the association and dissociation kinetics, it was also analyzed by the nonlinear regression method for statistical comparison to the other models. Model IV represents a combination of two noninterconvertible populations of receptors, one of which (R′) is incapable of coupling to an N protein and follows a mass action mechanism while the other (R) follows the complete cyclic ternary complex mechanism of DeLean et al. (1980). Models II and III include the "uncouplable" receptor (R′) combined with subsets of the ternary complex model in which the interaction of receptor (R) with N protein either occurs after (model II) or before (model III) agonist binding.

The three most complete sets of association kinetics (301 time points from three experiments each at 0.1, 0.3, and 1 nM, two experiments at 3 and 10 nM, and one experiment at 30 nM) were combined and fitted to each of the models under consideration. The number of independent kinetic parameters ranged from four in model I to nine in model IV. The receptor concentrations for each data set were also allowed to vary, introducing three additional free parameters. Two parameters were constrained in the initial fitting. The slow dissociation rate constant (i.e., k_{-1} in model I, k_{-2} in model II, and k_{-3} in models III and IV) was kept in the observed range [(2.8–4.3) × 10^{-4} s^{-1}]. The fraction of low-affinity receptor (R'/R_T) was fixed at 0.36 for all models in accord with the equilibrium binding data [Figure 3 and Neubig et al. (1985)].

Models II and IV gave the best fits upon analyzing the complete data set [sum of squared residuals (SS), 4.87 and 4.76, respectively]. Models I and III gave significantly greater residuals, 12.7 and 9.0, respectively ($p < 0.01$). There was deviation of the theoretical values from the data at the highest concentrations (10 and 30 nM) probably because different membrane and radioisotope dilutions were used. Consequently, we fit the data for the lower [^{3}H]UK 14 304 concentrations, 0.1–3 nM, to the models. Model II gave the best fit (SS 0.584) and model IV (SS 0.664) the next best (Figure 8). Models I and III again were significantly worse in fitting the data (SS 1.12 and 0.815, respectively) with p values of less than 0.01 compared to either model II or model IV. The parameters from fitting the partial data set were not substantially different from those with the whole set, so the latter were used. Thus, a ternary complex model which includes an interaction of agonist-occupied receptor (DR) with N protein provides the best quantitative approximation of α_2 agonist binding kinetics over a wide concentration range.

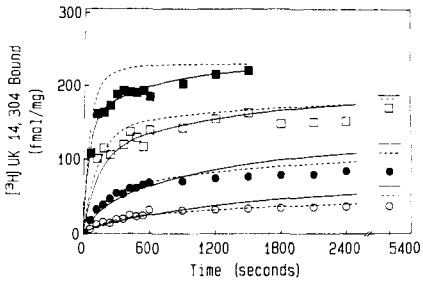

FIGURE 8: Nonlinear least-squares fits of [^{3}H]UK 14 304 association kinetics. Specific [^{3}H]UK 14 304 binding at concentrations of 0.1 (○), 0.3 (●), 1 (□), and 3 (■) nM is compared with theoretical predictions of model II (dashed line) and model IV (solid line). The parameter values for the two models were derived from fitting the entire association kinetic data set (301 time points). The parameters of model IV are shown in Table I.

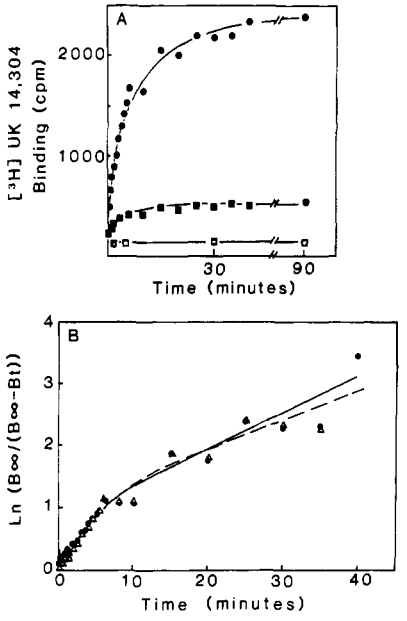

FIGURE 9: Kinetics of [^{3}H]UK 14 304 association in the presence and absence of GppNHp. (A) The time course of binding of 1 nM [^{3}H]UK 14 304 in the absence (●, ○) and presence (■, □) of 10^{-5} M GppNHp was measured as described in Figure 4 and under Materials and Methods. Nonspecific binding (○, □) was not affected by GppNHp. (B) Specific binding in the absence (●) of GppNHp was calculated as in Figure 4. Specific GppNHp-sensitive binding (△) was calculated by subtracting binding in the presence of GppNHp from binding in the absence of GppNHp for each time point. Semilogarithmic plots of specific binding in the absence (●) of 10^{-5} M GppNHp and calculated GppNHp-sensitive binding (△) are shown. Solid lines are theoretical curves for double-exponential processes with parameters obtained by nonlinear least-squares analysis of the data. Parameters for specific binding in the absence of GppNHp were A_f = 53%, k_f = 6.5 × 10^{-3} s^{-1}, and k_s = 0.98 × 10^{-3} s^{-1} and for GppNHp-sensitive binding were A_f = 65%, k_f = 4.8 × 10^{-3} s^{-1}, and k_s = 0.77 × 10^{-3} s^{-1}. These data are single (0–5 min) or duplicate (5–40 min) values from one experiment which has been performed 3 times with comparable results.

Effects of Guanine Nucleotides on [^{3}H]UK 14 304 Association and Dissociation. Of the two models that best fit the α_2 agonist association kinetics, only model IV predicts that the DRN complex will be included in the fast component of agonist binding. In order to assess the role of N proteins in the fast and slow agonist binding, we studied the effect of a saturating amount of guanine nucleotide (10 μM GppNHp) on [^{3}H]UK 14 304 binding kinetics. First, we measured the association kinetics of 1 nM [^{3}H]UK 14 304 in the presence and absence of nucleotide. The equilibrium binding was reduced by 80 ± 3% by nucleotide (Figure 9A). The time course of binding in the presence of GppNHp was fast, but

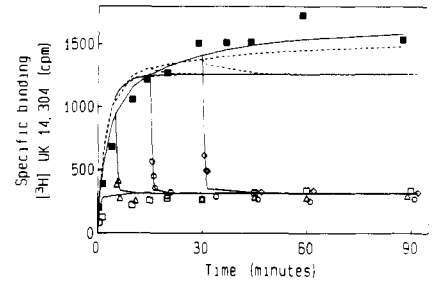

FIGURE 10: Effect of GppNHp on [^{3}H]UK 14 304 binding prior to equilibrium. Two nanomolar [^{3}H]UK 14 304 was mixed with an equal volume of prewarmed platelet membranes (0.175 mg/mL). At the indicated times, 1-mL aliquots were removed, diluted in 5 mL of TM buffer, and filtered. Nonspecific binding was determined in parallel samples to which 2 × 10^{-5} M oxymetzaoline had been added to the membranes prior to prewarming. Nonspecific binding was 320 cpm and was not affected by GppNHp. Specific binding in the absence (■) and presence (□) of 10^{-5} M GppNHp is shown. At five (△), 15 (○), and 30 (◇) min after binding was initiated, GppNHp was added to give a final concentration of 10^{-5} M. Specific binding was measured at 0.5, 1, 1.5, and 5 min and the additional indicated times after addition of nucleotide. Theoretical simulations of the experiment according to the parameters determined for model IV (solid lines) and model II (dashed lines) are shown.

the small amount of binding (100–400 cpm) precluded a detailed analysis. "Guanine nucleotide sensitive binding" accounted for approximately 80% of total binding and was defined as [^{3}H]UK 14 304 binding in the absence of nucleotide minus binding in the presence of nucleotide for each time (i.e., binding in the presence of nucleotide was used to define "nonspecific" binding). A semilogarithmic plot comparing total specific [^{3}H]UK 14 304 binding (filled circles) and guanine nucleotide sensitive binding (open triangles) is shown in Figure 9B. The nucleotide-sensitive binding exhibits fast and slow components nearly identical with those seen for total specific binding [A_f = 45 ± 18%, k_f = (8.6 ± 5.8) × 10^{-3} s^{-1}, and k_s = (0.61 ± 0.17) × 10^{-3} s^{-1}; n = 3]. Thus it appears that both the fast and the slow binding of [^{3}H]UK 14 304 involve α_2 receptor–N protein interactions. Indeed, all of the slow binding and a substantial amount of the fast binding are eliminated in the presence of 10 μM GppNHp.

To more directly assess the contribution of N proteins to the fast binding, we measured the effect of GppNHp on [^{3}H]UK 14 304 binding prior to equilibrium. Figure 10 shows that 10 μM GppNHp added 5, 15, or 30 min after [^{3}H]UK 14 304 was mixed with platelet membranes produced a prompt reduction in binding to the level seen when GppNHp was added before the agonist. To test the predictions of models II and IV with respect to effects of guanine nucleotides, we performed a simulation of this experiment using the SAAM modeling program. To model the effects of addition of nucleotide, the concentration of N protein was reduced to zero, the DRN complex was rapidly converted to DR, and the simulation was allowed to proceed. With the parameters for models II and IV which best fit the association kinetics, model IV accurately predicted the binding time course in the presence of nucleotide (Figure 10, solid line). Model II failed to account for the marked decrease in the equilibrium binding and, in fact, predicted a further increase in agonist binding when nucleotide was added at the preequilibrium times (Figure 10, dashed line). These results suggest that model IV best accounts for both the association time course and the nucleotide effects on agonist binding. The guanine nucleotide sensitivity of the fast [^{3}H]UK 14 304 binding indicates that there is a substantial "precoupling" of the platelet α_2 receptor with an N protein prior to agonist binding. Thus, a complete cyclic ternary complex model (i.e., model IV) is necessary to account for our

data.

Discussion

In this paper we present a detailed study of the kinetics of agonist and antagonist binding to α_2 adrenergic receptors. The goal of these experiments was to utilize information obtained from the time course of ligand binding to suggest models of the interaction of α_2 adrenergic receptors with the intracellular effector system. This is one of the first applications of such an approach to adenylate cyclase linked receptors in membranes. From these data we conclude that approximately one-third of the α_2 adrenergic receptor in human platelet membranes is unable to couple to N proteins, one-third is coupled prior to agonist binding, and another one-third becomes coupled upon addition of agonist. Rate constants for the interaction of liganded and unliganded α_2 receptors with the N protein are estimated.

The binding of the antagonist [^{3}H]yohimbine appears to be relatively simple. The time course of binding is well described by a single exponential process over a 30-fold range of concentrations. In addition, the secondary plot of k_{obsd} versus [^{3}H]yohimbine concentration is linear, and the equilibrium dissociation constant calculated from the derived forward and backward rate constants is in good agreement with the directly determined K_d. However, two features suggest that the binding of [^{3}H]yohimbine may not be completely described by a simple bimolecular association reaction. First, the association rate constant determined from these studies is 2.5×10^5 M^{-1} s^{-1}. This is more than 3 orders of magnitude lower than the theoretical diffusion limit for a bimolecular reaction in aqueous solution, 10^9 M^{-1} s^{-1}. It is possible that this discrepancy is due to the fact that the α_2 receptor is membrane bound, but association rate constants much closer to the diffusion limit have been observed for other membrane receptors. An association rate constant of 3×10^7 M^{-1} s^{-1} was reported for the nicotinic acetylcholine receptor at 4 °C (Boyd & Cohen, 1980a,b) as was a rate constant of 1.5×10^7 M^{-1} s^{-1} for the insulin receptor at 24 °C (Cuatrecasas, 1971). The second aspect of the data that is not entirely consistent with a simple bimolecular association model is the nonzero intercept for the semilogarithmic plot at 30 nM [^{3}H]yohimbine (Figure 1A). Though the deviation from zero is small (0.15), this observation was consistent, and preliminary data at higher [^{3}H]yohimbine concentrations have revealed an even larger deviation. The combination of a slow association rate constant and a rapid component of binding at higher ligand concentrations (i.e., the nonzero intercept) is suggestive of a conformational change in the receptor. Attempts to provide further evidence for an antagonist-induced conformational change by studying the preequilibrium dissociation kinetics, though, have not confirmed this possibility (Figure 2).

The results reported here for [^{3}H]yohimbine kinetics are similar to the limited information available in the literature. In the only study to report the rate of [^{3}H]yohimbine association at more than one concentration, Woodcock and Johnson (1982) obtained a forward rate constant of 5.2×10^5 M^{-1} s^{-1}. These authors utilized rat renal cortical membranes and [^{3}H]yohimbine over a concentration range of 1–5 nM. In several studies on human platelet membranes, similar forward rate constants were estimated from association kinetics determined at a single [^{3}H]yohimbine concentration (Garcia-Sevilla et al., 1981; Limbird et al., 1982). Thus the antagonist kinetics appear most consistent with a bimolecular binding mechanism with a slow rate constant, but further studies of the discrepancies indicated above may elucidate more complex aspects of the mechanism of [^{3}H]yohimbine binding.

Table I: Nonlinear Least-Squares Fitted Parameters for Model IV[a]

parameter	statistical fit	measured value	experimental procedure
k_1 (M^{-1} s^{-1})	3.2×10^6		
k_{-1} (s^{-1})	0.11		
K_{d1} (nM)	33	41	UK competition for yohimbine binding (+GppNHp)[b]
k_2N (s^{-1})	9.5×10^{-3}		
k_{-2} (s^{-1})	3.2×10^{-5}		
k_3	4.0×10^6		
k_{-3} (s^{-1})	4.3×10^{-4}[c]	$(2.8–4.3) \times 10^{-4}$	slow UK dissociation
K_{d3} (nM)	0.11		
k_4N (s^{-1})	3.5×10^{-4}		
k_{-4} (s^{-1})	2.6×10^{-4}		
K_d(app) (nM)	0.19	0.46 ± 0.13	equilibrium UK binding (high affinity)
k_1' (M^{-1} s^{-1})	7.2×10^6		
k_{-1}' (s^{-1})	0.017	0.01–0.02	fast UK dissociation
K_{d1}' (nM)	2.4	9.9 ± 7.8	equilibrium UK binding (low affinity)
R'/R_T	0.36[c]	0.36	equilibrium binding

[a] The best fitting parameters for [^{3}H]UK 14 304 binding according to model IV are indicated. Definitions of the parameters are as in Chart I. Experimental measurements which independently provide estimates of the parameters are also shown. The rates for the receptor–N protein interaction k_2 and k_4 are expressed as first-order rate constants in which the N protein concentration is included. This assumes only that the available N protein concentration is constant during the experiment. K_d(app) (see text footnote 3) indicates the apparent affinity of the agonist for couplable α_2 receptor. It includes contributions from K_{d1}, K_{d3}, k_4N, and k_{-4}. [b] Neubig et al. (1985). [c] Constrained to measured value.

As might be expected from the complex equilibrium binding of α_2 agonists, the kinetics of binding of [^{3}H]UK 14 304 are much more complex than those observed for [^{3}H]yohimbine. At no concentration of the full agonist was the binding time course exponential. The nonhyperbolic equilibrium binding rules out models including a single receptor undergoing a ligand-promoted conformational change since such models invariable predict hyperbolic equilibrium binding functions (Boyd & Cohen, 1980a; Weiland & Oswald, 1985). The same is true for the ternary complex model in the presence of excess N protein (Wreggett & DeLean, 1984; Neubig et al., 1985; Ehlert, 1985; Lee et al., 1986). The model which best accounted for the [^{3}H]UK 14 304 equilibrium binding and the association and preequilibrium dissociation kinetics was model IV. This model is a combination of an "uncouplable" low-affinity receptor binding agonist by a mass action mechanism (R′) and another form of the receptor (R) which interacts with N_i by a cyclic ternary complex mechanism.

In this model a receptor conformational change or coupling to N_i occurs *prior* to ligand binding at low agonist concentrations. As discussed by others (Lancet & Pecht, 1976; Boyd & Cohen, 1980a; Weiland & Oswald, 1985), such models result in slow rate constants which are nearly independent of ligand concentration as seen here. The GppNHp-sensitive, slowly dissociating component of the fast [^{3}H]UK 14 304 binding can be accounted for by the rapid binding of agonist to the preexisting RN complex.

The parameters derived from the nonlinear least-squares analysis of the association kinetic data are shown in Table I. Several of the parameters estimated from the fitting of the association kinetics have also been determined independently from dissociation or equilibrium binding experiments. The low-affinity binding in the absence of GppNHp was estimated

by nonlinear least-squares regression to a two binding site model[3] to have a K_d of 9.9 ± 7.8 nM (Figure 3). The fitted value of 2.4 nM is within that relatively large range. The equilibrium binding of [^{3}H]UK 14304 in the presence of GppNHp has been determined both directly (Figure 3) and by competition methods (Neubig et al., 1985). The direct method revealed a K_d of 6.8 nM, but only 44% of the [^{3}H]-yohimbine sites were detected. These values are similar to the fitted value of K_{d1}' and the percentage of R'. The competition data, with a K_d of 41 nM, appear to predominantly reflect the binding to R for which the fitted value is 33 nM. The rate constant for the fast [^{3}H]UK 14304 dissociation also agrees well with the fitted value of k_{-1}'. The predicted value of the overall high-affinity binding constant, K_d(app), is 0.19 nM. Although we have a relatively accurate experimental determination of this value, the fitted value is out of the measured range. The discrepancy is less than a factor of 2.5, but it suggests that either the estimate of the affinity of R for N, k_4/k_{-4}, or the affinity of ligand for the RN complex, K_{d3}, is off by a small amount.

The extent of coupling of receptors (R), guanine nucleotide binding proteins (N), and the catalytic subunit of adenylate cyclase in membranes has been an unresolved question. In detergent solutions there is considerable evidence for an R–N complex (Limbird et al., 1980; Smith & Limbird, 1981; Michel et al., 1981). Solubilization of membrane proteins in the absence of agonist results in loss of subsequently measured high-affinity agonist binding while preincubation of membranes with agonist prior to solubilization results in high-affinity agonist binding being retained. Methods to determine the state of interaction of R, N, and C in membranes are much less well developed. Radiation inactivation (Schlegel et al., 1979), kinetic modeling of adenylate cyclase activation (Tolkovsky et al., 1982), modeling of the equilibrium binding of agonists and antagonist (Wreggett & DeLean, 1984; Ehlert, 1985), and trapping of a putative receptor–N protein complex (Nerme et al., 1985) have all been used. It has been suggested on the basis of equilibrium binding studies that the state of coupling of R and N may depend on the type of receptor and conditions of the assay, including the type of cation present (Na^+ versus $Tris^+$) (Ehlert, 1985). Coupling of muscarinic acetylcholine receptors to N may be favored by the presence of Tris and the absence of Na^+. D_2 dopamine receptors may be coupled even in the presence of Na^+ (Wreggett & DeLean, 1984). The conditions of our measurements (Tris buffer with Na^+ absent) are those that have been suggested to favor coupling of muscarinic receptors and N. According to our results using binding kinetics, the fraction of "couplable" receptor (R) that is precoupled is equal to $k_4N/(k_4N + k_{-4})$ or 0.57. This corresponds to 37% of the total α_2 receptor population. The excellent fit of the effect of GppNHp on preequilibrium [^{3}H]UK 14304 binding strongly supports the existence of the precoupled RN complex.

Since agonist binds to RN 300-fold more tightly than to R, the interaction of agonist-occupied receptor with N protein must be of similarly higher affinity. The values of k_4N and k_2N in this model indicate that agonist increases the rate of association of R and N, and those for k_{-4} and k_{-2} indicate that agonist slows RN dissociation. The association is increased 30-fold and the dissociation decreased 10-fold. Although the estimates of k_4 and k_{-4} are probably more reliable than those for k_2 and k_{-2}, the changes are large enough to be significant.

The estimated values of the bimolecular rate constants for [^{3}H]UK 14304 [(3–7) × 10^6 M^{-1} s^{-1}] are more than an order of magnitude faster than that observed for [^{3}H]yohimbine. They are only a factor of 2–4 less than the bimolecular association rate constants seen for acetylcholine binding to nicotinic receptors (Boyd & Cohen, 1980a,b) and nitrendipine binding to calcium channels (Weiland & Oswald, 1985). We cannot resolve the fast phase of binding into multiple components even using rapid mix quench techniques (Neubig & Thomsen, 1987), providing additional evidence that all of these processes have rate constants close to 5 × 10^6 M^{-1} s^{-1}. Thus, the fast phase of [^{3}H]UK 14304 binding appears consistent with a bimolecular interaction of ligand with the preexisting receptor conformations.

The exact mechanism of the slow, ligand-independent step in [^{3}H]UK 14304 binding cannot be definitively specified. The ligand-independent step could be due to a slow diffusional interaction of the receptor and N protein; however, the rate constant of approximately 10^{-3} s^{-1} ($T_{1/2}$ = 690 s) observed for the slow binding is less than that expected for a pure diffusional interaction. Assuming a platelet surface area of 14 μm^2, 270 receptors per platelet (McFarlane & Stump, 1982), a 50-fold excess of N (Neubig et al., 1985), and a membrane vesicle radius of 0.1 μm,[4] there would be on average 120 N_i proteins and 2.4 receptors per vesicle. Even when a relatively low diffusion constant of 2 × 10^{-11} cm^2/s similar to that measured for band 3 protein (Fowler & Branton, 1977) and estimated for the turkey erythrocyte β adrenergic receptor (Hanski et al., 1979) is used combined with a small target size of 5 Å, a diffusion time constant of 31 s (k = 32 × 10^{-3} s^{-1}) is obtained from eq 4 of Rhodes et al. (1985). This assumes perfect irreversible trapping of the proteins, so a diffusional interaction with significant orientational constraints or incomplete trapping could possibly account for the slow binding kinetics. We have recently completed studies of the dependence of the fast and slow rate constants for [^{3}H]UK 14304 binding on temperature (Gantzos & Neubig, 1988). The slow rate constant is much more temperature sensitive than the fast rate constant, and an Arrhenius plot of the slow rate shows a "break" at 17 °C, the phase transition temperature of platelet membrane lipids (Lohse et al., 1986). These data are consistent with the hypothesis that the fast binding depends on diffusion in an aqueous environment while the slow phase depends on protein translation in a membrane environment. Additional studies involving alterations of the concentration of the receptor and N protein, or other approaches to alter the membrane environment, to change the rate of R and N interactions may be necessary to provide conclusive evidence for a diffusional basis for the slow ligand binding. The studies reported here provide the experimental paradigm for testing these hypotheses.

The results in this paper relate to the N protein dependent high-affinity binding of α_2 agonists to their receptor. The functional significance of this high-affinity binding has not been definitively established. For many N protein coupled receptors it has been suggested that the high-affinity N protein linked receptor conformation is the funtionally important one (Stadel et al., 1980). Arguments have also been made that the low-affinity receptor is functionally active (Ross et al., 1977), largely based on the correlation between the low-affinity binding constants and the effective concentrations of agonist

[3] In the presence of excess N, model IV predicts an *equilibrium* binding function that follows a two-site mass action equation. The low-affinity dissociation constant is K_{d1}'. The high-affinity equilibrium binding constant is

$$K_d(\text{app}) = K_{d3}(1 + k_4N/k_{-4})/(k_4N/k_{-4} + K_{d1}/K_{d3})$$

[4] M. Zamorski and R. R. Neubig, unpublished observations.

in functional studies. In pre-steady-state studies of α_2-mediated inhibition of platelet adenylate cyclase, we have found evidence that the high-affinity receptor conformation is the one linked to receptor function.[5] Thus the mechanism of receptor–N protein interactions studied in this paper is likely to be related to receptor function.

The studies reported here represent one of the first applications of a kinetic analysis of adrenergic agonist binding in membranes. The binding kinetics provide much more detailed information regarding the receptor mechanism than does equilibrium binding alone. The results suggest that the fast component of agonist binding is due in part to precoupled RN complex and the slow component of binding is due to a ligand-independent conformational transition of the α_2 adrenergic receptor that may be related to a diffusional interaction of receptor and N_i. This approach to the study of N protein linked receptors should prove to be a useful tool for gaining a better understanding of agonist–receptor–effector interactions.

Acknowledgments

We thank Olga Szamraj for assistance during the early stages of this project, Linda Harbison and Linda Busha for preparing the manuscript, and Dr. Harvey Motulsky for critically reviewing it.

Registry No. UK 14304, 59803-98-4; GppNHp, 34273-04-6; yohimbine, 146-48-5.

References

Asano, T., & Ross, E. M. (1984) *Biochemistry 23*, 5467–5471.

Asano, T., Pedersen, S. E., Scott, C. W., & Ross, E. M. (1984) *Biochemistry 23*, 5460–5467.

Boston, R. C., Greif, P. C., & Berman, M. (1981) *Comp. Prog. Biomed. 13*, 111–119.

Boyd, N. D., & Cohen, J. B. (1980a) *Biochemistry 19*, 5344–5353.

Boyd, N. D., & Cohen, J. B. (1980b) *Biochemistry 19*, 5353–5358.

Brandt, D. R., & Ross, E. M. (1986) *J. Biol. Chem. 261*, 1656–1664.

Bruns, R. F., Lawson-Wendling, K., & Pugsley, T. A. (1983) *Anal. Biochem. 132*, 74–81.

Cerione, R. A., Staniszewski, C., Benovic, J. L., Lefkowitz, R. J., Caron, M. G., Gierschik, P., Somers, R., Spiegel, A. M., Codina, J., & Birnbaumer, L. (1985) *J. Biol. Chem. 260*, 1493–1500.

Cerione, R. A., Regan, J. W., Nakata, H., Codina, J., Benovic, J. L., Gierschik, P., Somers, R. L., Spiegel, A. M., Birnbaumer, L., Lefkowitz, R. J., & Caron, M. D. (1986) *J. Biol. Chem. 261*, 3901–3909.

Cuatrecasas, P. (1971) *Proc. Natl. Acad. Sci. U.S.A. 68*, 1264–1268.

Czerlinki, G. H. (1966) *Chemical Relaxation*, Dekker, New York.

DeLean, A., Stadel, J. M., & Lefkowitz, R. J. (1980) *J. Biol. Chem. 255*, 7108–7117.

DeLean, A., Rouleau, D., & Lefkowitz, R. J. (1983) *Life Sci. 33*, 943–954.

DeMeyts, P., Bianco, A. R., & Roth, J. (1976) *J. Biol. Chem. 251*, 1877–1888.

Ehlert, F. J. (1985) *Mol. Pharmacol. 28*, 410–421.

Faden, V. B., & Rodbard, D. (1975) *EXPFIT, Exponential Data Processing*, BTIC Computer Code Collection, Biomedical Computing Technology Information Center, Vanderbilt Medical Center, Nashville, TN.

Ferscht, A. (1977) *Enzyme Structure and Mechanism*, pp 126–133, Freeman, San Francisco.

Florio, U. A., & Sternweis, P. C. (1985) *J. Biol. Chem. 260*, 3477–3483.

Fowler, V., & Branton, D. (1977) *Nature (London) 268*, 23–26.

Galper, J. B., & Smith, T. W. (1979) *Proc. Natl. Acad. Sci. U.S.A. 75*, 5831–5835.

Gantzos, R. D., & Neubig, R. R. (1988) *Biochem. Pharmacol.* (in press).

Garcia-Sevilla, J. A., Hollingsworth, P. A., & Smith, C. B. (1981) *Eur. J. Pharmacol. 74*, 329–341.

Gilman, A. G. (1984) *Cell (Cambridge, Mass.) 36*, 577–579.

Hanski, E., Rimon, G., & Levitzki, A. (1979) *Biochemistry 18*, 846–853.

Heidmann, T., Bernhardt, J., Neumann, E., & Changeux, J.-P. (1983) *Biochemistry 22*, 5452–5459.

Horwitz, E. M., Jenkins, T., Hoosein, N. M., & Gurd, R. S. (1985) *J. Biol. Chem. 260*, 9307–9315.

Hoyer, D., Renyolds, E. E., & Molinoff, P. B. (1984) *Mol. Pharmacol. 25*, 209–218.

Insel, P. H., Mahan, L. C., Motulsky, H. J., Stolman, L. M., & Koachman, A. M. (1984) *J. Biol. Chem. 258*, 13957–13605.

Jakobs, K.-H., & Aktories, K. (1983) *Biochim. Biophys. Acta 732*, 352–358.

Kim, M. H., & Neubig, R. R. (1985) *FEBS Lett. 192*, 321–325.

Kim, M. H., & Neubig, R. R. (1987) *Biochemistry 26*, 3664–3675.

Lancet, D., & Pecht, I. (1976) *Proc. Natl. Acad. Sci. U.S.A. 73*, 3549–3553.

Lee, T. W. T., Sole, M. J., & Wells, J. W. (1986) *Biochemistry 25*, 7009–7020.

Limbird, L. E., Gill, D. M., & Lefkowitz, R. J. (1980) *Proc. Natl. Acad. Sci. U.S.A. 77*, 775–779.

Limbird, L. E., Speck, J. L., & Smith, S. K. (1982) *Mol. Pharmacol. 21*, 609–617.

Loftus, D. J., Stolk, J. M., & U'Prichard, D. C. (1984) *Life Sci. 35*, 61–69.

Lohse, M. J., Klotz, K.-N., & Schwabe, U. (1986) *Mol. Pharmacol. 29*, 228–234.

Lowry, O., Rosebrough, N., Farr, A., & Randall, R. J. (1951) *J. Biol. Chem. 193*, 265–275.

May, D. C., Ross, E. M., Gilman, A. G., & Smigel, M. D. (1985) *J. Biol. Chem. 260*, 15829–15833.

McFarlane, D. E., & Stump, D. C. (1982) *Mol. Pharmacol. 22*, 574–579.

Michel, T., & Lefkowitz, T. J. (1982) *J. Biol. Chem. 257*, 13557–13563.

Michel, T., Hoffman, B. B., Lefkowitz, R. J., & Caron, M. G. (1981) *Biochem. Biophys. Res. Commun. 100*, 1131–1136.

Motulsky, H., & Insel, P. (1983) *FEBS Lett. 164*, 13–16.

Motulsky, H. J., & Mahan, L. C. (1984) *Mol. Pharmacol. 25*, 1–9.

Murayami, T., & Ui, M. (1984) *J. Biol. Chem. 259*, 761–769.

Nerme, V., Severne, Y., Abrahamsson, T., & Vauquelin, G. (1986) *Mol. Pharmacol. 30*, 1–5.

Neubig, R. R., & Szamraj, O. (1986) *Biochim. Biophys. Acta 854*, 67–76.

Neubig, R. R., & Thomsen, W. J. (1987) in *Membrane Proteins: Proceedings of the Membrane Protein Sympo-*

[5] W. J. Thomsen and R. R. Neubig, unpublished observations.

sium, Aug 3–6, 1986, San Diego, CA, Bio-Rad Laboratories, Richmond, CA.
Neubig, R. R., Boyd, N. D., & Cohen, J. B. (1982) *Biochemistry 21*, 3460–3467.
Neubig, R. R., Gantzos, R. D., & Brasier, R. S. (1985) *Mol. Pharmacol. 28*, 475–486.
Rhodes, D. G., Sariento, J. G., & Herbette, D. G. (1985) *Mol. Pharmacol. 27*, 612–623.
Rodbard, D. (1974) *Clin. Chem. 20*, 1255–1270.
Ross, E. M., Maguire, M. E., Sturgill, T. W., Biltonen, R. L., & Gilman, A. G. (1977) *J. Biol. Chem. 252*, 5761–5775.
Schlegel, W., Kempner, E. S., & Rodbell, M. (1979) *J. Biol. Chem. 254*, 5168–5176.
Schwartz, K. P., Lanier, S. M., Carter, E. A., Graham, R. M., & Hor, C. J. (1985) *FEBS Lett. 187*, 205–210.
Severne, Y., Ijzerman, A., Nerme, U., Timmerman, H., & Vauquelin, G. (1987) *Mol. Pharmacol. 31*, 69–73.
Smith, S. K., & Limbird, L. E. (1981) *Proc. Natl. Acad. Sci. U.S.A. 78*, 4026–4030.
Stadel, J. M., DeLean, A., & Lefkowitz, R. J. (1982) *Adv. Enzymol. Relat. Areas Mol. Biol. 53*, 1–43.
Stiles, G. L., Caron, M. G., & Lefkowitz, R. J. (1984) *Physiol. Rev. 64*, 661–745.
Strickland, S., Palmer, G., & Massey, V. (1975) *J. Biol. Chem. 250*, 4048–4052.
Toews, M. L., Harden, T. K., & Perkins, J. P. (1983) *Proc. Natl. Acad. Sci. U.S.A. 80*, 3553–3557.
Tolkovsky, A. M., & Levitzki, A. (1978) *Biochemistry 17*, 3795–3810.
Tolkovsky, A. M., Braun, S., & Levitzki, A. (1982) *Proc. Natl. Acad. Sci. U.S.A. 79*, 213–217.
Turner, J. T., Ray-Prenger, C., & Bylund, D. B. (1985) *Mol. Pharmacol. 28*, 422–430.
U'Prichard, D. C., Mitrius, J. C., Kahn, D. J., & Perry, B. D. (1983) in *Molecular Pharmacology of Neurotransmitter Receptors* (Sagawa, T., et al., Eds.) pp 53–72, Raven, New York.
Weiland, G. A., & Molinoff, P. B. (1981) *Life Sci. 29*, 313–330.
Weiland, G. A., & Oswald, R. E. (1985) *J. Biol. Chem. 260*, 8456–8464.
Woodcock, E. A., & Johnston, C. I. (1982) *Mol. Pharmacol. 22*, 589–594.
Wreggett, K. A., & DeLean, A. (1984) *Mol. Pharmacol. 26*, 214–227.

Rapid Lateral Diffusion of the Variant Surface Glycoprotein in the Coat of *Trypanosoma brucei*†

Roland Bülow,‡ Peter Overath,*,‡ and Jean Davoust§

Max-Planck-Institut für Biologie, Corrensstrasse 38, 7400 Tübingen, FRG, and European Molecular Biology Laboratory, Postfach 10.2209, 6900 Heidelberg, FRG

Received July 13, 1987; Revised Manuscript Received November 19, 1987

ABSTRACT: The membrane form of the variant surface glycoprotein (mfVSG) is anchored in the plasma membrane of *Trypanosoma brucei* by a dimyristoylphosphatidylinositol residue connected via a glycan to the COOH-terminal amino acid. The glycoprotein molecules are tightly packed, forming a coat that is impenetrable to lytic serum components. Lateral diffusion of mfVSG was measured by the fluorescence recovery after photobleaching technique. mfVSG labeled on the cell surface with rhodamine-conjugated anti-VSG Fab fragments showed a diffusion coefficient of 1×10^{-10} cm^2/s at 37 °C and of 0.7×10^{-10} cm^2/s at 27 °C. About 80% of the molecules were mobile. Affinity-purified mfVSG molecules implanted into the plasma membrane of baby hamster kidney cells exhibited a similar mobility to that found in the trypanosome coat [$D = (0.4–0.7) \times 10^{-10}$ cm^2/s at 4 °C]. Phospholipid mobility in the plasma membrane of trypanosomes was characterized by a diffusion coefficient of 2.2×10^{-9} cm^2/s at 37 °C. It is concluded that mfVSG mobility in the surface coat of the parasite is rapid and comparable to that of other membrane-bound glycoproteins but slower than that of phospholipids.

African trypanosomes, exemplified by *Trypanosoma brucei*, are unicellular eucaryotic flagellates that parasitize the blood and tissues of their mammalian host. The entire cell surface is covered by a coat that consists of a single glycoprotein species, designated the variant surface glycoprotein (VSG). Every cell has the potential to express a large number of different VSG's, thereby enabling the parasite to evade the host's immune response (Borst, 1986).

About 10^7 VSG molecules are considered to be arranged at the surface of each cell in a tightly packed single layer of homodimers separated by a mean distance of about 40 Å (Cross, 1975; Auffret & Turner, 1981; Freymann et al., 1984; Jackson et al., 1985). The N-terminal two-thirds of the molecule form a domain that carries the antigenic determinants accessible to antibodies in live cells. Although the amino acid sequence of the N-terminal domain from different VSG's is not homologous, all of these proteins, nevertheless, appear to assume a similar, rodlike shape that is attributable to a bundle of four long α-helices per dimer (Freymann et al., 1984; Metcalf et al., 1987; Jähnig et al., 1987). VSG's are anchored in the membrane by a dimyristoylphosphatidylinositol residue connected via a glycan and an ethanolamine to the COOH terminus (Holder, 1983; Ferguson & Cross, 1984; Ferguson et al., 1985; Jackson & Voorheis, 1985). In this membrane

† This work was supported by the Fond der Chemischen Industrie.
‡ Max-Planck-Institut für Biologie.
§ European Molecular Biology Laboratory.

0006-2960/88/0427-2384$01.50/0